

# Origin of chaos in nuclear spectra: role of symmetries

T. Papenbrock <sup>a,b</sup> and H. A. Weidenmüller <sup>c</sup>

<sup>a</sup>*Physics Division, Oak Ridge National Laboratory, Oak Ridge, TN 37831, USA*

<sup>b</sup>*Department of Physics and Astronomy, University of Tennessee,  
Knoxville, TN 37996, USA*

<sup>c</sup>*Max-Planck-Institut für Kernphysik, D-69029 Heidelberg, Germany*

---

## Abstract

We investigate the role of symmetry as a possible origin of chaos in the nuclear shell model. For this purpose we disentangle purely geometrical effects due to spin and isospin coupling of the many-body states, from effects of the reduced two-body interaction. We compare a model without symmetry (the embedded two-body ensemble of random matrices) with the two-body random ensemble (TBRE) of the shell model. We show that in the TBRE, there is already considerable mixing of many-body states from only a single reduced two-body matrix element. This is particularly the case for a single  $j$ -shell and, in a shell model with subshells, for the many-body states which belong to the same partition (same number of nucleons in each of the subshells). We conclude that in the shell model, chaos is largely generated by symmetry. This mechanism differs considerably from that of the embedded ensemble.

*Key words:* Shell Model, Symmetry, Complexity

*PACS:* 21.10.-k, 05.45.Mt, 24.60.-k

---

## 1 Introduction and Motivation

The analysis of nuclear spectra has produced ample evidence for chaotic motion. Indeed, near neutron threshold, the spectra of medium-weight and heavy nuclei display fluctuations which agree with those of random matrices drawn from the Gaussian orthogonal ensemble (GOE) [1]. Similar agreement has been found for nuclei in the  $sd$ -shell (both in experimental data [2] and in shell-model calculations [3]), and in the ground-state domain of heavier nuclei [4], although here there exists strong evidence, too, for regular motion as predicted by the shell model and the collective models. Calculations in Ce [5]

have produced similar evidence for chaotic motion in atoms. Thus, chaos appears to be an ubiquitous feature of interacting many-body systems. What is the origin of this behavior? This is the question we address in the present Letter.

We do so using the nuclear shell model, a theory with a mean field and a residual two-body effective interaction  $V$ . (We do not include three-body forces, although there is evidence [6] that these may be needed to attain quantitative agreement with data. It will be seen that qualitatively, our arguments would not change with the inclusion of such forces.) In many nuclei, the mean field is (nearly) spherically symmetric. Thus, single-particle motion is largely regular. Chaos in nuclei seems a generic property and, hence, must be due to  $V$ . We focus attention entirely upon the effects of  $V$ . Therefore, we assume that we deal with a single major shell in which the single-particle states are completely degenerate. (A lack of complete degeneracy would reduce the mixing of states due to  $V$  and, thus, drive the system towards regular motion). Generic results are expected to be independent of the details of  $V$ . Therefore, we assume that the two-body matrix elements (TBME) of  $V$  are uncorrelated Gaussian-distributed random variables with zero mean value and unit variance. Our results then apply to almost all two-body interactions with the exception of a set of measure zero. (The integration measure is the volume element in the parameter space of the TBME.)

The two-body interaction  $V$  has two characteristic features. (i) It connects pairs of nucleons. (ii) It possesses symmetries: it conserves spin, isospin, and parity. To elucidate the roles played by both features in producing chaos in nuclei, we compare two different models for the two-body interaction. In both models,  $m$  fermions are distributed over  $l > m$  degenerate single-particle states. Hilbert space is spanned by the resulting  $N = \binom{l}{m}$  Slater determinants. The two-body interaction connects only those Slater determinants which differ in the occupation numbers of not more than two single-particle states. The first model is the embedded two-body ensemble of Gaussian orthogonal random matrices (EGOE(2)) [7]. For a recent review we refer the reader to ref. [8]. This model does not respect the symmetries of the shell model. Neither the single-particle states nor  $V$  carry any quantum numbers. The representation of  $V$  in Hilbert space yields a sparse matrix (most non-diagonal matrix elements vanish) and is very different from a typical realization of the GOE which has non-zero matrix elements between every pair of states. The second model is the two-body random ensemble (TBRE) [9,10]. Here, the single-particle states carry spin, isospin, and parity quantum numbers, and  $V$  conserves these symmetries. Hilbert space decays into orthogonal subspaces carrying these same quantum numbers. Each subspace is spanned by states which are linear combinations of (many) Slater determinants. As a result, the matrix representation of  $V$  in any such subspace becomes fairly dense, even though it remains true that  $V$  connects only Slater determinants which differ

in the occupation numbers of not more than two single-particle states. We show that both in the  $sd$ -shell and in a single  $j$ -shell, the TBRE does generically lead to chaos. (This aspect of the TBRE has been coined ‘‘geometric chaoticity’’ by Zelevinsky *et al.* [3]. To the best of our knowledge, however, the actual role of symmetries in producing chaos in nuclei has never been investigated.) We conclude that symmetry directly causes chaos in nuclear spectra. We now investigate both models in detail.

## 2 Absence of Symmetries

In the absence of symmetries, the appropriate model is the EGOE(2). The EGOE(2) is often used to model stochastic aspects of realistic systems like small metallic grains or quantum dots. This is justified since in those systems the single-particle wave functions themselves are chaotic, and the resulting two-body matrix elements reflect this property and transport the information of the underlying one-body chaos into the many-body system. Several numerical studies for matrix dimensions up to a few thousand or so have shown that the EGOE(2) exhibits GOE statistics in the center of the spectrum. For infinite matrix dimensions, the situation is less clear. Evidence from previous work on the EGOE(2) [11,12] suggests that the level statistics is Poissonian. However, no firm conclusion has yet been reached [13]. Here, we supplement the previous analysis by a different approach and focus on the matrix structure. In the EGOE(2), the random variables are the  $a = \binom{l}{2}[\binom{l}{2} + 1]/2$  independent two-body matrix elements  $V_\alpha$ ,  $\alpha = 1, \dots, a$ . A Hamiltonian drawn from the EGOE(2) has matrix elements

$$H_{\mu\nu} = \sum_{\alpha=1}^a V_\alpha D_{\mu\nu}(\alpha) , \quad (1)$$

where the matrices  $D_{\mu\nu}(\alpha)$  transport the information contained in the two-body matrix elements  $V_\alpha$  into the  $N$ -dimensional Hilbert space spanned by Slater determinants labeled  $\mu$  or  $\nu$ . The ensemble average of the Hamiltonian is obviously zero. The second moment is

$$\overline{(H_{\mu\nu})^2} = \sum_{\alpha} (D_{\mu\nu}(\alpha))^2 . \quad (2)$$

The properties of the matrices  $D_{\mu\nu}$  are obtained by counting. Let  $\mu$  and  $\nu$  differ in the occupation numbers of  $f$  single-particle states. (a) If  $f \geq 3$ , then  $\sum_{\alpha} (D_{\mu\nu}(\alpha))^2 = 0$ . (b) If  $f = 2$ , then  $\sum_{\alpha} (D_{\mu\nu}(\alpha))^2 = 1$ . (c) If  $f = 1$ , then  $\sum_{\alpha} (D_{\mu\nu}(\alpha))^2 = (m - 1)$ . (d) If  $f = 0$  or  $\mu = \nu$ , then  $\sum_{\alpha} (D_{\mu\mu}(\alpha))^2 = \binom{m}{2}$ . For the number of times each of these alternatives is realized, we find (a)

$\sum_{j \geq 3} N \binom{m}{j} \binom{l-m}{j}$ , (b)  $N \binom{m}{2} \binom{l-m}{2}$ , (c)  $Nm(l-m)$ , and (d)  $N$ . The number of zero matrix elements dominates (it is close to  $N^2$ ). The number of unit values comes next and is approximately  $(1/4)Nm^2(l-m)^2$ . The number of values  $(m-1)$  is  $Nm(l-m)$ . The number of values  $\binom{m}{2}$  is trivially equal to  $N$ , the dimension of the matrix and the number of diagonal elements. The correlators  $\sum_{\alpha} D_{\mu\nu}(\alpha)D_{\rho\sigma}(\alpha)$  can also be worked out easily but are not given here. They do not all vanish. Therefore, the random variables  $V_{\alpha}D_{\mu\nu}(\alpha)$  are not independent.

The individual matrices  $D_{\mu\nu}(\alpha)$  have a very simple structure and barely mix many-body states. Let the TBME corresponding to index  $\alpha$  change the occupation of  $f$  particles. For  $f = 0$  the matrix  $D_{\mu\nu}(\alpha)$  is diagonal. For  $f = 1, 2$  the matrix  $D_{\mu\nu}(\alpha)$  can be ordered to have  $\binom{l-2-f}{m-2}$  block matrices of dimension two and is zero otherwise. This shows that individual matrices  $D_{\mu\nu}(\alpha)$  cannot generate mixing and chaos.

We consider the limit of large matrix dimension  $N$ , attained by taking the limit  $l \rightarrow \infty$ . This can be done in two ways: (i) by keeping the ratio  $m/l$  fixed; (ii) by keeping  $m$  fixed. (i) The ratio of the number of non-diagonal elements with variance unity to the total number of matrix elements is  $(1/4)m^2(l-m)^2/N$ . This ratio tends to zero as  $l \rightarrow \infty$ . The same ratio calculated for the non-diagonal elements with variance  $(m-1)$  vanishes even faster. The correlators of the diagonal elements are  $\sum_{\alpha} D_{\mu\mu}(\alpha)D_{\nu\nu}(\alpha) = \binom{k}{2}$  where  $k$  is the number of single-particle states that are occupied in both  $\mu$  and  $\nu$ . The correlation is maximal for  $k = m-1$  and vanishes for  $k = 0$  and  $k = 1$ . For fixed  $\mu$  and  $k$ , the number of states  $\nu$  for which the occupation of  $k$  single-particle states is the same as in  $\mu$  is  $\binom{l-m}{m-k} \binom{m}{k}$ . For  $k = m-1$ , this yields  $m(l-m)$  and for  $k = 1$ , we find  $m \binom{l-m}{m-1}$ . The ratio of both expressions to  $N$  vanishes exponentially fast as  $l \rightarrow \infty$ . Thus, the matrices approach diagonal form with uncorrelated diagonal elements that all have the same variance. This is suggestive of the Poissonian distribution. (ii) The ratio of the number of non-diagonal elements with variance unity to the total number of matrix elements is  $(1/4)m^2l^2/N$  and vanishes exponentially fast. The same holds true *a fortiori* for the elements with variance  $m-1$ . Again, the correlators of the diagonal elements are given by  $\binom{k}{2}$ , and the number of states which correlate to a given one with this correlator is  $\binom{l-m}{m-k} \binom{m}{k}$ . The ratio of this value to  $N$  vanishes as a power of  $l$ . Again, this is suggestive of the Poissonian distribution. We note, however, that sparseness of a random matrix is no guarantee for Poissonian statistics. Indeed, Fyodorov and Mirlin [14] have shown that sparse random matrices with *uncorrelated* non-vanishing matrix elements that have a frequency  $p/N$  and no preference for large diagonal elements may have either Poissonian or GOE statistics, depending on the value of  $p$ . While these results are quite suggestive, the question about spectral fluctuations of the EGOE(2) in the limit of large matrix dimension remains open.

We apply these considerations to the half-filled  $sd$ -shell. The number of single-particle states is  $l = 24$ ; the number of nucleons is  $m = 12$ . The number of independent TBME is  $a \approx 3.8 \times 10^4$ . The corresponding matrices of the embedded ensemble have dimension  $N \approx 2.7 \times 10^6$ . The variance of the diagonal elements is 66. The fraction of non-diagonal elements with variance unity is approximately  $1.9 \times 10^{-3}$ , that of those with variance  $m - 1 = 11$  is approximately  $5.3 \times 10^{-5}$ . The Hamiltonian matrices of the EGOE(2) are thus characterized by their sparsity, strong diagonal structure, and a relatively large number of independent TBME.

### 3 Presence of symmetries

As mentioned above, diagonalization of shell-model matrices does often lead to GOE-type spectral fluctuations; see, for instance, Ref. [3]. In the TBRE, we distribute  $m$  valence nucleons over  $q$  single-particle subshells with total angular momenta  $j_k, k = 1, \dots, q$ . To simplify the notation, we drop the parity quantum number. The many-body states  $\mu, \nu$  have spin and isospin quantum numbers  $J$  and  $T$ , respectively. The spin-isospin coupled reduced TBME  $V^{st}(j_k, j_l; j_m, j_n)$  (with  $k \leq l, m \leq n$ , and  $s$  and  $t$  the two-body spin and isospin, respectively) are labeled  $V_\alpha, \alpha = 1, \dots, a$  where  $a$  depends upon the particular shell under consideration. The shell-model Hamiltonian has matrix elements

$$H_{\mu\nu}^{JT} = \sum_{\alpha=1}^a V_\alpha C_{\mu\nu}^{JT}(\alpha) . \quad (3)$$

Again, the matrices  $C_{\mu\nu}^{JT}(\alpha)$  transport the information about the TBME  $V_\alpha$  into the many-body states. In contrast to the EGOE(2), these matrices are now determined by both the spin-isospin symmetry and the fermionic nature of the  $m$ -body system. Each element is given in terms of sums over products of angular-momentum coupling coefficients, and coefficients of fractional parentage and is thus a rather complex quantity. The properties of the matrices  $C_{\mu\nu}^{JT}(\alpha)$  thus cannot be inferred as easily as those of the matrices  $D_{\mu\nu}$  in Eq. (2). To understand the structure of these matrices, we use first a qualitative analysis. Our analysis applies to the  $sd$ -shell and to other shells with more than one subshell in heavier nuclei. The case of a single  $j$ -shell differs from these cases and is treated below. We label the  $JT$ -coupled many-body basis states by the occupation numbers  $(n_1, \dots, n_q)$  of the  $q$  subshells. Here  $(n_1, \dots, n_q)$  is a partition of  $m$  into  $q$  integers, so that  $\sum_{k=1}^q n_k = m$ . We assume that the many-body basis states belonging to a given set of quantum numbers  $JT$  are ordered in blocks, each block containing states belonging to the same partition. The reduced TBME fall into two classes. The first class consists of the

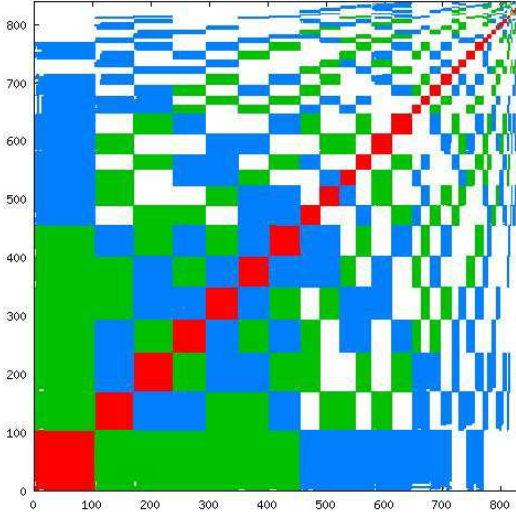


Fig. 1. Non-zero matrix elements of the  $sd$ -shell many-body Hamiltonian with  $m = 12$  nucleons (“ $^{28}\text{Si}$ ”) in the sector  $J = T = 0$ . Matrix elements originating from diagonal reduced two-body matrix elements are red. Matrix elements originating from off-diagonal reduced two-body matrix elements that transfer one (two) particles between partitions are green (blue).

“diagonal” reduced TBME  $V^{st}(j_k, j_l; j_k, j_l)$ . These couple only states within the same partition. The matrices  $C_{\mu\nu}(\alpha)$  corresponding to these TBME are block-diagonal. The second class consists of the “off-diagonal” reduced TBME  $V^{st}(j_k, j_l, j_m, j_n)$  with  $(j_k, j_l) \neq (j_m, j_n)$ . These TBME change the occupation numbers  $(n_1, \dots, n_q)$  and thus couple different partitions. Among these off-diagonal TBME there are those with  $k \neq m, n$  and  $l \neq m, n$ , and those with  $k = m$ , or  $k = n$ , or  $l = m$ , or  $l = n$ . The former (latter) change the occupation numbers of the subshells by two (one) unit, respectively. The matrices  $C_{\mu\nu}(\alpha)$  corresponding to these off-diagonal reduced TBME have non-zero entries in the off-diagonal blocks only. As a result, the matrix  $H_{\mu\nu}^{JT}$  attains a checker-board pattern which reflects the partitions. The pattern is that of  $m$  *bosons* distributed over  $q$  single-particle orbitals that interact via two-body interactions.

We show this structure for the particular case of the  $sd$ -shell with  $l = 24$  single-particle states,  $q = 3$  subshells with  $j_1 = d_{5/2}, j_2 = d_{3/2}, j_3 = s_{1/2}$ , occupation numbers  $n_1, n_2, n_3$ , and a total of 41 partitions. Among the  $a = 63$  reduced TBME, 28 are diagonal, 22 of the off-diagonal reduced TBME induce one-body transitions between the partitions, and 13 transfer two particles. We consider the case of  $m = 12$  nucleons (“ $^{28}\text{Si}$ ”) in the sector  $J = T = 0$ . The resulting matrix has dimension 839. All calculations were done using the shell model code OXBASH [15]. Figure 1 shows the matrix structure (non-zero matrix elements only) of a generic Hamiltonian (3). The partition structure and the resulting checker-board pattern are clearly visible.

To elucidate further the structure of the shell–model Hamiltonian of Eq. (3), we ask: How many matrices  $C_{\mu\nu}(\alpha)$  yield a non–zero contribution to a given matrix element  $H_{\mu\nu}^{JT}$ ? A matrix element of the diagonal blocks gets on average non–zero contributions from  $25.2 \pm 4.0$  of the 28 block–diagonal matrices corresponding to the diagonal reduced TBME. For the off–diagonal–block matrices corresponding to off–diagonal reduced TBME, the numbers are  $7.2 \pm 1.4$  out of 22 and  $2.0 \pm 0.9$  out of 13 for those transferring one and two particles between different partitions, respectively. This shows that in its non–zero blocks, each of the individual matrices  $C_{\mu\nu}(\alpha)$  is rather densely populated, and that the density decreases with an increasing number of transferred particles.

Further insight into the structure of the Hamiltonian (3) is obtained when we confine attention to the block–diagonal matrices  $C_{\mu\nu}(\alpha)$  associated with diagonal TBME. We diagonalize these matrices and compute the average number of principal components ( $NPC$ ), i.e. the inverse of the sum over the expansion coefficients raised to the fourth power [3], for each partition. The average is taken over all eigenstates within one partition and over the ensemble of block–diagonal matrices  $C_{\mu\nu}(\alpha)$  and is shown in Table 1. We recall that for the GOE and in the limit of infinite matrix dimension  $D$ , the value would be  $NPC/D = 1/3$ : a typical GOE eigenstate has significant overlap with about 1/3 of the basis states. Table 1 shows that  $NPC/D$  amounts to between 25% and 70% of the GOE expectation for the partitions with dimension  $D > 20$ . The partitions with smaller dimensions yield even higher values for  $NPC/D$ , but the fluctuations typically increase with decreasing dimension. The degree of mixing tends to decrease with increasing dimension of the partitions although there are considerable fluctuations. We conclude that each diagonal reduced TBME thoroughly mixes the states belonging to a fixed partition. To fully appreciate these statements, the reader should recall that the matrices  $C_{\mu\nu}(\alpha)$  do not carry any specific information on the two–body interaction and are determined exclusively by the symmetries of the problem (exclusion principle and conserved quantum numbers  $J$  and  $T$ ). The mixing within each partition is expected to be even stronger when we consider a generic two–body interaction and the resulting superposition of matrices  $C_{\mu\nu}(\alpha)$  in Eq. (3).

Although the mixing between partitions is not as strong as that within each partition,  $H_{\mu\nu}^{JT}$  will, for  $^{28}\text{Si}$  and  $J = 0$   $T = 0$ , generically generate chaos. To show this, we have compared our Figure 1 with the corresponding figure for the Wildenthal two–body interaction (which was used in Ref. [3] and shown there to produce chaos; see, e.g., Figs. 23(a) and 23(c) of that reference). The two figures are indistinguishable.

We also investigate the TBRE for the case of a single  $j$ –shell with  $m = 6$  fermions and  $j = 19/2$ . This is a shell model with a single partition. Our earlier results then suggest strong mixing of states. There are  $a = j + 1/2 = 10$  TBME as two particles can have spins  $s = 0, 2, 4, \dots, (j - 1)/2$ . The cor-

Partition	$D$	$NPC/D$
(6, 4, 2)	103	0.10
(7, 3, 2)	67	0.11
(5, 5, 2)	67	0.14
(5, 4, 3)	56	0.18
(7, 4, 1)	56	0.09
(6, 3, 3)	53	0.15
(6, 5, 1)	53	0.13
(8, 2, 2)	35	0.20
(4, 6, 2)	35	0.21
(4, 5, 3)	34	0.23
(8, 3, 1)	34	0.14
(7, 2, 3)	27	0.22
(5, 6, 1)	27	0.24

Table 1

Number of principal components  $NPC$  normalized by the dimension  $D$  for the 13 largest partitions generated by mixing due to the block-diagonal matrices  $C_{\mu\nu}(\alpha)$ . The GOE expectation for infinite matrix dimension is  $1/3$ .

responding spin-conserving two-body operators are denoted by  $\hat{V}_s$ . Diagonalizing  $\hat{V}_s$  is tantamount to diagonalizing the corresponding matrix  $C_{\mu\nu}(s)$ . Hilbert space is spanned by Slater determinants of single-particle states. These have spin projection  $J_z = 0$  (but not well-defined total spin  $J$ ) and are labeled  $|\mu\rangle$  with  $\mu = 1, \dots, D = 1242$ . The eigenstates of  $\hat{V}_s$  are written as  $|s, J, i\rangle = \sum_{\mu=1}^D c_{\mu}(s, J, i)|\mu\rangle$ . Here  $i = 1, \dots, d_J$  where  $d_J$  is the dimension of the subspace of states with spin  $J$ . The complexity of the eigenstates  $|s, J, i\rangle$  is measured by the number of principal components

$$(NPC)^{-1} = \sum_{\mu=1}^D c_{\mu}^4(s, J, i). \quad (4)$$

Table 2 shows the  $NPC$ s, averaged over all two-body spins  $s$  and over all  $d_J$  states with spin  $J$ . We recall that the GOE expectation is  $NPC/D = 1/3$ . We see that the spin-conserving two-body operators  $\hat{V}_s$  individually yield a strong mixing of the basis states. This mixing is purely due to the rotational symmetry and independent of any particular choice of the two-body interaction. It may be argued that the complexity of the coefficients  $c_{\mu}(s, J, i)$  reflects just the need to couple the states  $|\mu\rangle$  to total spin  $J$ , and is not indicative

of strong mixing due to  $\hat{V}_s$ . Inspection of the individual coefficients  $c_\mu(s, J, i)$  shows, however, strong variations with the index  $s$ , which invalidates this argument. Moreover, calculation of the  $NPCs$  in a basis with fixed  $J$  confirms our picture.

$J$	$d_J$	$NPC/D$	$J$	$d_J$	$NPC/D$	$J$	$d_J$	$NPC/D$
0	10	0.27	1	6	0.27	2	23	0.24
3	21	0.23	4	37	0.24	5	32	0.24
6	49	0.24	7	43	0.24	8	56	0.25
9	51	0.25	10	62	0.25	11	54	0.25
12	65	0.26	13	56	0.26	14	63	0.26
15	55	0.26	16	60	0.26	17	50	0.26
18	55	0.26	19	45	0.26	20	47	0.27
21	39	0.26	22	40	0.27	23	31	0.26
24	33	0.26	25	25	0.26	26	25	0.26
27	19	0.24	28	19	0.24	29	13	0.23
30	14	0.24	31	9	0.22	32	9	0.21
33	6	0.21	34	6	0.21	35	3	0.20
36	4	0.20	37	2	0.18	38	2	0.17
39	1	0.16	40	1	0.15	42	1	0.13

Table 2

Number of principal components  $NPC$  normalized by the dimension  $D$  for a system of 6 fermions in a single  $j = 19/2$  shell. The  $NPCs$  are averaged over all two-body spins and over the  $d_J$  states with spin  $J$ . The GOE expectation for infinite matrix dimension is  $1/3$ .

#### 4 Discussion

There are both similarities and differences between the EGOE(2) and the TBRE. For matrix dimensions of up to a few thousand or so, matrices from both ensembles display GOE statistics in the center of the spectrum. However, both ensembles differ considerably in the way they generate mixing and chaos. In the EGOE(2), matrices corresponding to individual TBME have a very simple structure and mix only pairs of many-body states. Here, chaos is generated by the relatively large number of TBME and the resulting superposition of a correspondingly large number of individually simple matrices that form the Hamiltonian. For the TBRE, the situation is distinctly differ-

ent. The number of independent TBME is rather small, but the coupling to good spin and isospin leads to considerable mixing and complexity already for the matrices corresponding to an individual TBME. This is true especially for the case of a single  $j$ -shell, and for the “diagonal” TBME in the  $sd$ -shell. Here, a hallmark of the chaos-generating mechanism is the natural grouping of many-body states into partitions and the considerable pre-mixing that occurs within each partition, independently of any one-body interaction. Our results strongly suggest that chaos in the nuclear shell model is to a large extent caused by symmetry, and not by any particular properties of the effective two-body interaction.

## Acknowledgements

This research was supported in part by the U.S. Department of Energy under Contract Nos. DE-FG02-96ER40963 (University of Tennessee) and DE-AC05-00OR22725 with UT-Battelle, LLC (Oak Ridge National Laboratory).

## References

- [1] R. U. Haq, A. Pandey, and O. Bohigas, Phys. Rev. Lett. **48**, 1086 (1982); O. Bohigas, R. U. Haq, and A. Pandey, in *Nuclear Data for Science and Technology*, K. H. Böchhoff (Ed.), Reidel, Dordrecht (1983).
- [2] G. E. Mitchell, E. G. Bilpuch, P. M. Endt, and F. J. Shriner, Jr., Phys. Rev. Lett. **61**, 1473 (1988); F. J. Shriner, Jr., E. G. Bilpuch, P. M. Endt, and G. E. Mitchell, Z. Phys. A **335**, 393 (1990).
- [3] V. Zelevinsky, B. A. Brown, N. Frazier, and M. Horoi, Phys. Rep. **276**, 85 (1996).
- [4] A. Abul-Magd, M. Simbel, H.-L. Harney, and H. A. Weidenmüller, Phys. Lett. B **579**, 278 (2004), nucl-th/0212057.
- [5] V. V. Flambaum, A. A. Gribakina, G. F. Gribakin, and M. G. Kozlov, Phys. Rev. A **50**, 267 (1994).
- [6] S. C. Pieper, R. B. Wiringa, Ann. Rev. Nucl. Part. Sci. **51**, 53 (2001), nucl-th/0103005.
- [7] K. K. Mon and J. B. French, Ann. Phys. (NY) **95**, 90 (1975).
- [8] V. K. B. Kota, Phys. Rep. **347**, 223 (2001).
- [9] J. B. French and S. S. M. Wong, Phys. Lett. B **33**, 449 (1970).
- [10] O. Bohigas and J. Flores, Phys. Lett. B **34**, 261 (1971).

- [11] L. Benet, T. Rupp, H. A. Weidenmüller, Phys. Rev. Lett. **87**, 010601 (2001), cond-mat/0010425; Ann. Phys. **292**, 67 (2001), cond-mat/0010426.
- [12] L. Benet and H. A. Weidenmüller, J. Phys. A **36**, 3569 (2003), cond-mat/0207656.
- [13] M. Srednicki, Phys. Rev. E **66**, 046138 (2002), cond-mat/0207201.
- [14] Y. V. Fyodorov und A. D. Mirlin, J. Phys. A **24**, 2273 (1991).
- [15] B. A. Brown, A. Etchegoyen, and W. D. M. Rae, *The computer code OXBASH*, MSU-NSCL report number 524 (1988).